doi:10.3788/gzxb20164504.0405001

基于多阶频率栅格的湍流相位屏低频补偿

马雪莲,喇东升

(东北大学 秦皇岛分校 计算机与通信工程学院,河北 秦皇岛 066004)

摘 要:提出一种基于多阶频率栅格划分的子谐波方法用于湍流相位屏的构造.通过对相位屏频域空间划分多阶频率栅格,并将每一阶的频率栅格进行更进一步精细子划分,补偿对湍流谱贡献最多的低频范围频率分量.采用大气湍流的相位结构函数和功率谱分析所构造相位屏的准确度.仿真结果表明:由所构造相位屏得到的相位结构函数与由湍流谱直接计算得到的理论值之间的偏差随着频率栅格总阶数 M、每一阶的频率栅格点数目 N_x' 和 N_y' 的增大而减小,对每一组 M、N_x'、N_y' 的取值,子划分前的频率间隔 Δf_1 有一最佳值;当选取 $M=3$、$N_x'=N_y'=3$、$\Delta f_1=2\ \mathrm{m}^{-1}$ 时,所构造的相位屏的相位结构函数和功率谱与理论十分接近;所产生的随机相位屏的整体倾斜反映了低频成分的准确采样.

关键词:大气光学;大气湍流;相位屏;子谐波;频率栅格

中图分类号:TN929.12 **文献标识码**:A **文章编号**:1004-4213(2016)04-0405001-9

Low Frequency Compensation for Turbulent Phase Screen Based on Multi-order Frequency Grids

MA Xue-lian, LA Dong-sheng

(*School of Computer and Communication Engineering, Northeastern University at Qinhuangdao, Qinhuangdao, Hebei* 066004, *China*)

Abstract: A subharmonic method was proposed based on the multi-order frequency grids dividing for the generation of the turbulent phase screen to compensate the low frequency components. Frequency grids were divided by multiple orders in the frequency domain of phase screen, and the frequency grids of each order were further finely subdivided, and then the frequency components in low frequency range which contribute the most to the turbulent spectrum could be compensated sufficiently. The phase structure function and the power spectrum of atmospheric turbulence were used to analyze the accuracy of the generated phase screen. Simulation results show that the discrepancy between the phase structure function derived from the generated phase screen and the theoretical value directly calculated from the turbulent spectrum is decreased by the increasing of the total number of frequency grid orders M, and frequency grid point number of each order $N_x'$and N_y'. For every group of M, $N_x'$and N_y', there is an optimum value for frequency space before subdividing Δf_1. By selecting $M=3$, $N_x'=N_y'=3$ and $\Delta f_1=2\ \mathrm{m}^{-1}$, the phase structure function and the power spectrum of the screen can be quite closely to theory. The overall slope in the generated random phase screen reflects an accurate sampling of the low frequency components.

Key words: Atmospheric optics; Atmospheric turbulence; Phase screen; Subharmonic; Frequency grid

OCIS Codes: 050.5080; 050.5082; 010.1290; 010.1330; 010.3310

Foundation item: The Fundamental Research Funds for the Central Universities (Nos. N110323006, N142303003) and the National Natural Science Foundation of China (No. 61501100)

First author: MA Xue-lian (1981—), female, lecturer, Ph. D. degree, mainly focuses on optical wave propagation through atmospheric turbulence, atmospheric laser communication and atmospheric laser imaging. Email: maxl@neuq.edu.cn

Received: Oct. 19, 2015; **Accepted**: Dec. 19, 2015

0 Introduction

Numerical simulation of the turbulence-induced wave front distortion is an important way for studying light propagating and imaging through atmospheric turbulence in many applications, such as near-earth laser communication[1-3], LADAR (Laser Detection and Ranging) imaging[4] and adaptive optics[5-7]. The split-step simulation method based on multiple random turbulent phase screens, first introduced by Fleck in 1976[8], has been widely developed by related researchers. In this method, the effect of atmospheric turbulence on light wave front can be regarded as a series of phase screens every certain distance located in the plane perpendicular to the propagation direction. The accurate generation of turbulent phase screen is investigated in numerical simulation of light propagating through atmospheric turbulence. Several methods have been used for generating a turbulent phase screen. A common method is based on the Fast Fourier Transform (FFT), in which phase screen is inversely Fourier-transformed from the power spectrum of turbulence[9-11]. Using Zernike polynomials and a series of random coefficients is another method to generate a phase screen[12-13]. Also, the correlation matrix method[14-15] can be used in some applications.

Among these phase screen generating methods, the FFT-based phase screen is most commonly used since it has the advantages of fast implementing and less memory requirement. However, directly using the FFT-based phase screen has a drawback of the loss of low frequency components. For a power spectrum of atmospheric turbulence, low frequency components provide a main contribution, so the loss of low components degrades the accuracy of the generated phase screen severely. In order to include more low-frequency components, a quite large phase screen is required by using FFT, which will increase the sample points while keeping a certain spatial resolution in space domain of phase screen, thus the amount of computing will be increased. Several subharmonic methods have been proposed to compensate the low frequency components without much computing amount[10,16]. In these subharmonic methods, low frequency components can be compensated by expanding phase screen or adding the subharmonic levels, and the statistical characteristics of simulated phase screen can be closer to that of the theoretical turbulence, as the size of the expanding screen increases or the number of subharmonic level increases.

Frequency grid dividing is very essential in subharmonic method, since frequency components contained in phase screen are dependent on frequency grids. Frequency grids of phase screen should be divided for every useful frequency section to match the power spectrum of atmospheric turbulence. We propose a subharmonic method based on multi-order frequency grid nesting to compensate low frequency components lost in the FFT-based phase screen. The frequency grid is subdivided finely for each order according to the power spectrum of atmospheric turbulence, and the phase structure function and power spectrum of generated phase screen are close to theory.

1 Subharmonic method for compensating low frequency loss in FFT-based phase screen

In the FFT-based phase screen which is commonly used in numerical simulation for light propagation through atmospheric turbulence, the loss of low frequency components is a problem. The subharmonic method is an effective solution to compensate the low frequency components.

A phase screen is constituted of turbulence-induced phase perturbations in the two dimensional (2D) plane perpendicular to the propagation direction. Phase screen is generated by inversely Fourier transforming on the power spectrum of atmospheric turbulence in the FFT-based method. The turbulence can be reasonably assumed to be isotropic and homogeneous, and the 2D power spectrum of atmospheric refractive-index fluctuation can be represented by the modified Von Kármán model including the influence of outer scale as follows[11]

$$\Phi_n(\kappa_r, z) = 0.033 C_n^2(z)(\kappa_r^2 + \kappa_0^2)^{-11/6} \tag{1}$$

where $\kappa_0 = 2\pi/L_0$, L_0 is the outer scale, $C_n^2(z)$ is the structure constant, and $\kappa_r = (\kappa_x^2 + \kappa_y^2)^{1/2}$ is the radial spatial wave number in the plane perpendicular to the propagation direction (z axis), in which $\kappa_x = 2\pi/x$ and $\kappa_y = 2\pi/y$ are the spatial wave numbers along x and y respectively.

Turbulent phase can be expressed as the integral of the refractive index along the path, so the 2D power spectrum of turbulent random phase can be written as

$$S_{\Delta\varphi}(\kappa_x, \kappa_y, z) = 2\pi k^2 \int_z^{z+\Delta z} \Phi_n(\kappa_r, z)\,\mathrm{d}\xi = 2\pi k^2 \cdot 0.033(\kappa_r^2 + \kappa_0^2)^{-11/6} \int_z^{z+\Delta z} C_n^2(\xi)\,\mathrm{d}\xi \tag{2}$$

By introducing the definition of atmospheric coherence length[17]

$$r_0 = 0.185\,(\lambda^2 / \int_z^{z+\Delta z} C_n^2(\xi)\,\mathrm{d}\xi)^{3/5} \tag{3}$$

Eq. (2) can be expressed by

$$S_{\Delta\varphi}(\kappa_r) = 0.490 r_0^{-5/3}(\kappa_r^2 + \kappa_0^2)^{-11/6} \tag{4}$$

where $\lambda = 2\pi/k$ is the optical wavelength. According to the 2D power spectrum of the random turbulent phase, the random phase in the 2D plane (x, y) can be obtained by[9, 11]

$$\Delta\varphi(x,y)=\int\int_{-\infty}^{\infty} g(\kappa_x,\kappa_y)\sqrt{S_{\Delta\varphi}(\kappa_x,\kappa_y)}\,\mathrm{e}^{\mathrm{i}\boldsymbol{\kappa}\times\boldsymbol{r}}\mathrm{d}\boldsymbol{\kappa} \quad (5)$$

where $g(\kappa_x,\ \kappa_y)$ is a Hermitian Gaussian white noise process.

The random phase screen is discrete in numerical simulation, and can be divided as a discrete rectangle grid structure with total size of $G_x\times G_y$, grid points of $N_x\times N_y$, and each grid size of $\Delta x\times\Delta y$. Each grid size which is also the spatial interval of two adjacent grid points can be derived by $\Delta x=G_x/N_x$ and $\Delta y=G_y/N_y$, along x and y respectively. The frequency space in frequency domain is the reciprocal of the total screen size as $\Delta f_x=1/G_x$ and $\Delta f_y=1/G_y$. The spatial frequency is related to the spatial wave number by $f_x=\kappa_x/2\pi$ and $f_y=\kappa_y/2\pi$. Spatial discrete points on phase screen can be represented as $x=0,\ \pm\Delta x,\ \cdots,\ \pm(N_x/2-1)\Delta x$ and $y=0,\ \pm\Delta y,\ \cdots,\ \pm(N_y/2-1)\Delta y$, and discrete frequency points in frequency domain can be represented as $f_x=0,\ \pm\Delta f_x,\ \cdots,\ \pm(N_x/2-1)\Delta f_x$ and $f_y=0,\ \pm\Delta f_y,\ \cdots,\ \pm(N_y/2-1)\Delta f_y$. By performing discrete operation on Eq. (5) and considering the scaling coefficient, the discrete phase distribution on phase screen can be expressed as[9, 11]

$$\Delta\varphi(p\Delta x,q\Delta y)=\sum_{m=-N_x/2}^{N_x/2-1}\sum_{n=-N_y/2}^{N_y/2-1}h(m\Delta f_x,n\Delta f_y)\cdot F_\varphi(m\Delta f_x,n\Delta f_y)\exp\left[2\pi\mathrm{i}(mp/N_x+nq/N_y)\right] \quad (6)$$

where p, q, m and n are all integers, $h(m\Delta f_x,\ n\Delta f_y)$ is a discrete Gaussian white noise process with zero-mean and unit-variance, and

$$F_\varphi(m\Delta f_x,n\Delta f_y)=2\pi\sqrt{\Delta f_x\Delta f_y}\,0.0024r_0^{-5/6}\times\left[(m\Delta f_x)^2+(n\Delta f_y)^2\right]^{-11/12} \quad (7)$$

Eq. (6) can be regarded as turbulent filter. The FFT which is the most effective Discrete Fourier transform (DFT) can be applied to realize the operation of Eq. (6). The result of $\Delta\varphi$ represents the random phase screen with discrete grid structure according to the refractive index power spectrum of atmospheric turbulence.

Frequency components contained in the FFT-based phase screen are determined by total size and spatial interval of phase screen. The maximum sample frequency can be derived from the spatial interval as $f_{x\max}=1/(2\Delta x)$ and $f_{y\max}=1/(2\Delta y)$. The sample frequency space is the reciprocal of the total screen size as $\Delta f_x={}_1/G_x$ and $\Delta f_y=1/G_y$. The minimum non-zero frequency is equal to the frequency space, *i.e.*, $f_{x\min}=\Delta f_x={}_1/G_x$ and $f_{y\min}=\Delta f_y=1/G_y$. It is noted that the sample at the origin $(f_x,\ f_y)=(0,\ 0)$ (the point with the frequency of zero) contributes the same average phase shift to every point in phase screen. Since this phase shift will not induce any distortion on the wave front, the sample of the zero frequency will not act on statistical characteristics of phase screen. Therefore, only the frequency range between the minimum non-zero frequency and the maximum frequency can be regarded as the effective frequency range in phase screen.

As we can see from the power spectrum of the refractive index according to the modified Von Kármán turbulence, the main contribution is located in the range of low frequency components close to $1/L_0$, whereas high-frequency components have little contribution since the spectrum amplitude decays quickly as the frequency increases. The outer scale L_0 with the value of several meters to tens of meters exhibits low frequency characteristics of atmospheric turbulence, such as tilt. If phase screen is not large enough to ensure that the minimum non-zero frequency is less than or close to $1/L_0$, the FFT-based phase screen cannot reflect low frequency characteristics due to low-frequency loss. In this case, low frequency effect of turbulence on the wave front such as tilt cannot be simulated accurately. Enlarging phase screen is a way to increase low frequency components in the FFT-based method. The whole screen size should be several times of L_0 as to guarantee sampling low frequency components sufficiently, and it is suggested that the screen size should achieve at least five times of the outer scale[9]. On the center region of phase screen, a high spatial resolution is required to ensure sufficient phase points acting on the beam. Only in this case the simulation for the effect of atmospheric turbulence on the propagating light can be accurate. In this case, the sample point number is large and the amount of computing will be evidently large for the FFT-based simulation.

The subharmonic method is employed to solve the problem of low frequency loss existing in the FFT-based phase screen. Two basic subharmonic methods are the two-order phase screen method proposed by Herman and Strugala[9], and the multiple 3×3 frequency grids method proposed by Lane, Glindemann and Dainty[10]. Johasson and Gavel present a subharmonic method which combines these two basic methods[11]. In these subharmonic methods, the larger the added low frequency screen is, or the more the subharmonic levels are, the closer to $1/L_0$ of the compensated frequency will be, hence the simulated result will be closer to the theoretical turbulence. The subharmonic method can compensate low frequency components while keeping a high resolution in phase screen center region covered by the light, and the amount of computing will not be so large. In this method, the center of phase screen keeps a high resolution, and a phase grid structure with large size and low resolution is added around the center screen.

The outer large screen contains sufficient low frequency components, so as called "low-frequency phase screen", whereas the center screen guarantees the sample resolution in the region covered by the light, containing high-frequency information, so as called "high-frequency phase screen". From the angle of frequency domain, several subharmonic levels in the form of low frequency grid points are added to high frequency grids.

Frequency grid dividing for phase screen is important in the subharmonic method. It is better to divide frequency grid finely enough according to the power spectrum of atmospheric turbulence, so as to ensure that the frequency range contributing the most to the turbulent spectrum can be sampled accurately. Phase screen accuracy can be enhanced by setting grid order number suitably, selecting low-frequency and high-frequency grids reasonably, and dividing each order finely. We propose a subharmonic method to compensate low frequency components lost in the FFT-based phase screen, based on multi-order frequency grids. For each order, the frequency grids are further finely subdivided.

2 The subharmonic method based on multi-order frequency grid dividing

On the basis of subharmonic principle, we propose a multi-order frequency grid dividing method for compensating the low frequency components. In this method, frequency grids are divided more finely in frequency domain according statistical characteristics of atmospheric turbulence. The detailed sample frequency distribution is shown in Fig. 1. The sample frequency distribution for generating phase screen is based on multi-order 3×3 frequency grids, and each grid for every order is subdivided into several smaller sub-grids. As the low frequency components take up the main part in turbulent spectrum and the spectrum amplitude decays quickly with the frequency rising, frequency grid dividing principle of the lower frequency being sampled more finely should hold. The high frequency information can be intercepted at a suitable maximum value, since enhancing the frequency can do little contribution to the spectrum when the frequency exceeds a certain value.

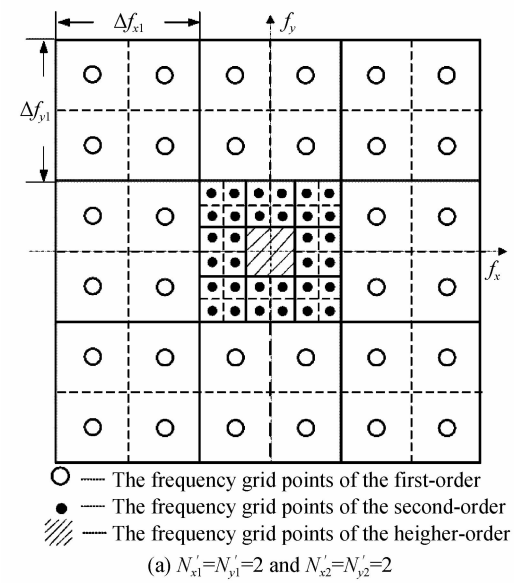

(a) $N'_{x1}=N'_{y1}=2$ and $N'_{x2}=N'_{y2}=2$

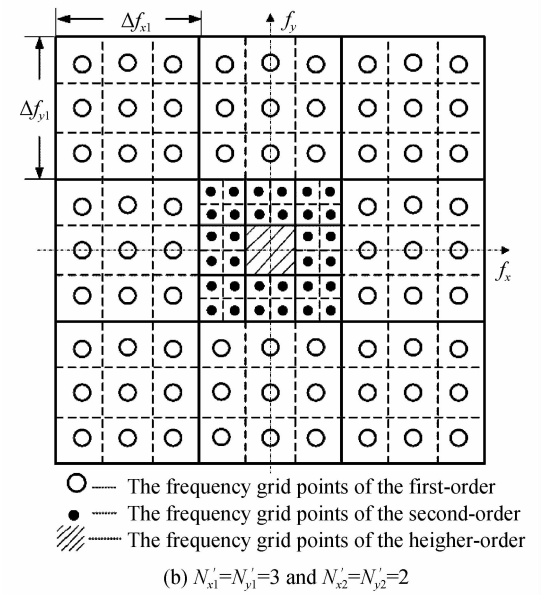

(b) $N'_{x1}=N'_{y1}=3$ and $N'_{x2}=N'_{y2}=2$

Fig. 1 Frequency distribution of multi-order frequency grid method

According to the required maximum frequency, we can choose a suitable frequency space Δf_{x1} and Δf_{y1} of the first order grids before further dividing. In the frequency domain, the first-order with 3×3 grids is divided, in which eight outer frequency grids are performed finely sampled. Each of the outer eight grids is subdivided into $N'_{x1} \times N'_{x1}$ sub-grid points, *i. e.*, every initial frequency grid contains a smaller frequency space. The remaining center grid (containing low frequency information around the zero-frequency) is divided into the second-order 3×3 grids, the outer eight grids of which are in turn subdivided in the same way as the first-order grids. The number of sub-grid points in each outer grid for the case of the second-order can be denoted as $N'_{x2} \times N'_{y2}$. The number of the sub-grid points selected for each order can be different or the same.

The above dividing process is repeated for adding the fine low-frequency sampling into the center grid in the form of 3×3 nesting with sub-grids. Every 3×3 grid dividing means one order. The outmost order is called the first-order, and the order number is in turn adding one for every inner 3×3 grids. The total order number of frequency grids is denoted by M. Fig. 1(a) shows the case of the same sub-grid point number for

each order with $N_{x1}^{'}=N_{y1}^{'}=2$ and $N_{x2}^{'}=N_{y2}^{'}=2$, and Fig. 1(b) shows the case of the different sub-grid point number for each order with $N_{x1}^{'}=N_{y1}^{'}=3$ and $N_{x2}^{'}=N_{y2}^{'}=2$. To simplify the problem, the same number as shown in Fig. 1(a) is employed, and the denotation of $N_x^{'}$ and $N_y^{'}$ are employed for unification.

The maximum frequency difference, the frequency space of each order, and the minimum non-zero frequency can be derived from the frequency grid dividing. The high frequency information is determined by the eight outer grids of the first order with the maximum frequency difference of $3\Delta f_{x1}$ and $3\Delta f_{y1}$. The frequency space for the mth-order is $\Delta f_{x1}/(3^{m-1}N_x^{'})$ and $\Delta f_{y1}/(3^{m-1}N_y^{'})$. The minimum non-zero frequency for $N_x^{'}$ and $N_y{}'$ being odd numbers is different from that for $N_x^{'}$ and $N_y^{'}$ being even numbers. When $N_x^{'}$ and $N_y^{'}$ are odd, the original point $(f_x, f_y)=(0, 0)$ on frequency grids is sampled but without any influence on the phase structure function, and the effective non-zero minimum frequency is located in the innermost Mth order and can be derived from $\Delta f_{x1}/(3^{M-1}N_x^{'})$ and $\Delta f_{y1}/(3^{M-1}N_y^{'})$. When $N_x^{'}$ and $N_y^{'}$ are even numbers, the original point $(f_x, f_y)=(0, 0)$ is not sampled, and the non-zero minimum frequency is $(1/2)\cdot\Delta f_{x1}/(3^{M-1}N_x^{'})$ and $(1/2)\cdot\Delta f_{y1}/(3^{M-1}N_y^{'})$. The phase screen can be expressed by the nesting form of

$$\Delta\varphi(x,y)=\sum_{m=0}^{M}\sum_{n_x^{'}=\mathrm{ceil}(-N_x^{'}/2)}^{\mathrm{ceil}(N_x^{'}/2-1)}\sum_{n_y^{'}=\mathrm{ceil}(-N_y^{'}/2)}^{\mathrm{ceil}(N_y^{'}/2-1)}h(n_x^{'},n_y^{'})\times F_\varphi(n_x^{'},n_y^{'})\mathrm{e}^{\mathrm{i}2\pi(f_x\cdot x+f_y\cdot y)} \tag{8}$$

where ceil (·) denotes rounding up to an integer, $h(n_x^{'}, n_y^{'})$ is a discrete white Gaussian process in the spectrum domain with zero-mean and unit-variance, and

$$F_\varphi(n_x^{'},n_y^{'})=2\pi\sqrt{\Delta f_x\Delta f_y}\,0.024r_0^{-5/6}\cdot(f_x^2+f_y^2)^{-11/12} \tag{9}$$

where

$$\Delta f_x=\Delta f_{x1}/(3^{m-1}N_x^{'}),\ \Delta f_y=\Delta f_{y1}/(3^{m-1}N_y^{'}) \tag{10}$$

and

$$\begin{cases} f_x=n_x^{'}\Delta f_x, f_y=n_y^{'}\Delta f_y & N_x^{'}\text{ and }N_y^{'}\text{ are odd} \\ f_x=(n_x^{'}+0.5)\Delta f_x, f_y=(n_y^{'}+0.5)\Delta f_y & N_x^{'}\text{ and }N_y^{'}\text{ are even} \end{cases} \tag{11}$$

It is worth noting that in space domain, the total size and sampling resolution of phase screen can be set according to the diameter of the beam propagating through atmospheric turbulence, therefore a very large screen in space domain is never actually needed. The points on phase screen in space domain can be set with the same interval, and there is no need to be the same nesting form as in frequency domain. The FFT cannot be directly used due to the irregular frequency grids, and only a general DFT can be applied in the method. Even though the DFT is not as effective as the FFT, the computing amount of the proposed subharmonic method can be still reduced compared with that of the method of directly generating the large phase screen based on the FFT, since this method needs fewer points.

As the frequency grids in each order are further subdivide, the frequency distribution of the phase screen can be set to match accurately with variation trend of turbulent spectrum, by adjusting the grid order number M, the original frequency space Δf_{x1} and Δf_{y1}, and the grid point number of each order $N_x^{'}\times N_y^{'}$. As long as the associated parameters are selected properly to ensure the frequency grids being divided close to turbulent spectrum, the frequency components can be adequately and accurately contained, and the phase screen can be produced very accurately in an efficient way, compared with the subharmonic methods in Refs. [9-11].

In our multi-order frequency grid subdividing method, for one sample point in space domain of phase screen, as there are nine frequency grids before subdiving, and there are $N_x^{'}\times N_y^{'}$ sub-grid points in each initial frequency grids, the computing amount for each order is $9N_x^{'}N_y^{'}$ by use of a DFT operation. For an order number of M, the computing amount is $9MN_x^{'}N_y^{'}$. If the sample point number needed for phase screen is $N_x\times N_y$ in space domain, the total computing amount is about $9MN_xN_yN_x^{'}N_y^{'}$. Note that the subharmonic components are added in a manner of irregularly spaced points for multiple orders. This can cause a ringing effect at the edge of the generated phase screen, so a phase screen at least twice the desired size should be produced and the central range of the phase screen is used to simulate the effect of atmospheric turbulence on the wavefront. As for a beam diameter of 50 cm, a screen size of $G_x\times G_y=1\ \mathrm{m}\times 1\ \mathrm{m}$ can be selected to satisfy the twice size of the beam diameter. For a resolution of 1 cm, the required number of the grid points is $N_x\times N_y=100\times 100$. For the case of $N_x^{'}\times N_y^{'}=3\times 3$ and $M=4$, which is sufficient to generate a very accurate phase screen, the computing amount is $9\times 4\times 100\times 100\times 3\times 3\approx 3.2\times 10^6$.

3 The accuracy of phase screen in terms of phase structure function and power spectrum

We use the phase structure function and the power

spectrum to analyze the accuracy of the phase screen generated by the proposed method. These two terms of the generated phase screen are compared with that of theoretical turbulence, and the accuracy is determined by the discrepancy between them.

The phase structure function is defined as the mean squared phase difference of two points with a certain distance on phase screen. Since atmospheric turbulence is assumed to be isotropic and homogeneous, the phase structure function is only related to the distance of the point pair, and defined by

$$D_\varphi(r)=[(\varphi(\boldsymbol{\rho}+\boldsymbol{r})-\varphi(\boldsymbol{\rho}))^2] \tag{12}$$

where r is the distance of two points on the phase screen. The phase structure function can be related to the 2D autocorrelation function $B_\varphi(r)$ by the expression of

$$D_\varphi(r)=2(B_\varphi(0)-B_\varphi(r)) \tag{13}$$

where the 2D autocorrelation function is defined by

$$B_\varphi(\boldsymbol{r})=[\varphi(\boldsymbol{\rho}+\boldsymbol{r})\varphi(\boldsymbol{\rho})]=\int_{-\infty}^{\infty}\int F_\varphi(\boldsymbol{\kappa})\mathrm{e}^{\mathrm{i}\boldsymbol{r}\cdot\boldsymbol{\kappa}}\mathrm{d}\boldsymbol{\kappa} \tag{14}$$

According to the modified Von Kármán model, the theoretical phase structure function of atmospheric turbulence with the outer scale L_0 can be expressed as[18]

$$D_\varphi(r)=6.16r_0^{5/3}\left[\frac{3}{5}\left(\frac{L_0}{2\pi}\right)^{5/3}-\frac{(rL_0/(4\pi))^{5/6}}{\Gamma(11/6)}\cdot K_{5/6}\left(\frac{2\pi r}{L_0}\right)\right] \tag{15}$$

where $K_{5/6}(\cdot)$ is the modified Bessel function of the third kind, and $\Gamma(\cdot)$ is the Gamma function.

One method for obtaining the phase structure function of the simulated phase screen is through evaluating the ensemble average of random phases[9]. Another method is to obtain the expected phase structure function through calculating the 2D discrete autocorrelation function by use of the 2D power spectrum[11]. We use the second method to calculate the expected phase structure function. The 2D discrete autocorrelation function for the phase screen generated by the proposed method can be expressed as

$$B_\varphi(x,y)=\sum_{m=0}^{M}\sum_{n_x'=\mathrm{ceil}(-N_x'/2)}^{\mathrm{ceil}(N_x'/2-1)}\sum_{n_y'=\mathrm{ceil}(-N_y'/2)}^{\mathrm{ceil}(N_y'/2-1)}F^2(n_x',n_y')\cdot \mathrm{e}^{\mathrm{i}2\pi(f_x\cdot x+f_y\cdot y)} \tag{16}$$

As we can see, the autocorrelation function expression does not contain Gaussian random variable $h(n_x', n_y')$ since what we desire is the expected value. The expected phase structure function can be calculated from the autocorrelation function through Eq. (13). The discrepancy of the simulated result with theory can reflect the accuracy of phase screen.

The performance of the phase structure function $D_\varphi(r)$ of the multi-order frequency grid dividing method and the theoretical result are given in Fig. 2 and Fig. 3. The outer scale of atmospheric turbulence is $L_0=10$ m, and atmospheric coherence length is $r_0=0.1$ m. The accuracy of the screen is related to the grid order number M, the frequency space before subdividing Δf_{x1} and Δf_{y1}, and the grid points of each order $N_x'\times N_y'$. As we can see, the screen accuracy is determined by the combination of these parameters. The case of $N_x'=N_y'=1$ without subdividing is shown in Fig. 2, and the case of $N_x'=N_y'=2$ and $N_x'=N_y'=3$ with subdividing is shown in Fig. 3(a) and (b),

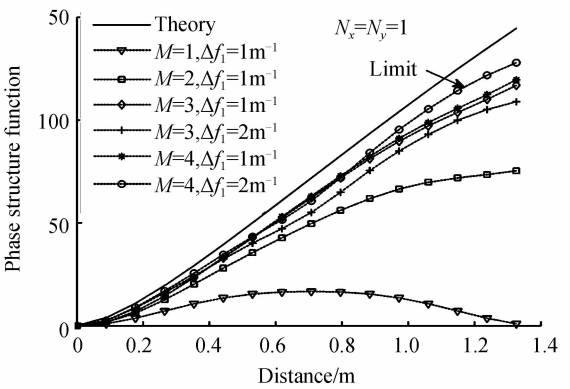

Fig. 2 Phase structure function of phase screen generated by multi-order frequency grid method without subdividing as $N_x'=N_y'=1$

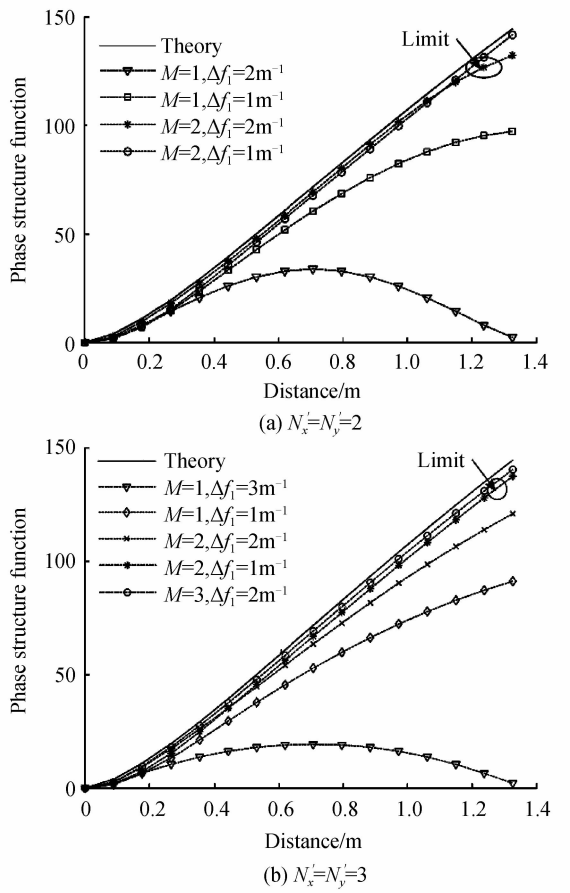

Fig. 3 Phase structure function of phase screen generated by multi-order frequency grid method with subdividing

respectively. For a certain $N_x' \times N_y'$, the screen accuracy is improved as the grid order number M increases, and when M arrives at a limit value, there is no further improvement. In this situation, adjusting the value of Δf_{x1} and Δf_{y1} can further improve the result, and hence an optimized performance can be achieved by choosing a suitable value of Δf_{x1} and Δf_{y1}. For simplification, we choose the same value for Δf_{x1} and Δf_{y1}, so a uniform denotation of Δf_1 instead of Δf_{x1} and Δf_{y1} is used in Fig. 2 and Fig. 3. The limit case marked in Fig. 2 and Fig. 3 individually reflects the best performance for a certain value of $N_{x\,a}'$nd N_y'.

For the case of $N_x' = N_y' = 1$, which means there is no subdividing in each grid for every order, we can see that the discrepancy between the simulated screen and theory always exists, and a best result achieves when $M = 4$ and $\Delta f_1 = 2\ \mathrm{m}^{-1}$, as illustrated in Fig. 2. Even in this condition, the discrepancy is still evident. This demonstrates that frequency grids without further subdividing will not achieve an optimal performance. The simulated phase structure function will be improved when $N_x' = N_{y=}' 2$ and $N_x' = N_y' = 3$ since further subdividing is implemented. In the case of $N_x' = N_y' = 2$ as shown in Fig. 3(a), when $M = 2$, and $\Delta f_1 = 1\ \mathrm{m}^{-1}$ or $\Delta f_1 = 2\ \mathrm{m}^{-1}$, the simulated phase structure function is extremely close to theory, which means the phase screen is accurate sufficiently. The same situation occurs when $M = 2$ and $\Delta f_1 = 1\mathrm{m}^{-1}$, or $M = 3$ and $\Delta f_1 = 2\mathrm{m}^{-1}$ in the case of $N_x' = N_y' = 3$ as shown in Fig. 3(b), and rather better than the former, the simulated curve is smoothly close to theory.

For comparison, Fig. 4 shows the phase structure functions of our multi-order method and the conventional subharmonic method presented by Lane *et al.* in Ref. 10. In Fig. 4, curve a represents the phase structure of our multi-order method, in which the parameters are selected as $M = 3$, $N_x' = N_y' = 3$, and $\Delta f_1 = 2\ \mathrm{m}^{-1}$, while curve b represents the phase structure of the subharmonic method by Lane *et al.* in Ref. 8, in which eight subharmonic levels is selected. Two curves both represent the most accurate case for each method. As we can see, the phase structure function of our method can achieve a more accurate value, which corresponds to a more accurate phase screen.

The radial power spectrum of the generated phase screen $S_{\Delta\varphi}'(\kappa_r)$can be calculated by performing Fourier-Bessel transform on the autocorrelation function through the relation of

$$S_{\Delta\varphi}'(\kappa_r) = \frac{1}{2\pi}\int_0^{\infty} B_\varphi(r)\mathrm{J}_0(n\kappa_r)r\mathrm{d}r \tag{17}$$

where $\mathrm{J}_0(\cdot)$ is the zero-order Bessel function of the first kind. The discrete autocorrelation function can be obtained by Eq. (16), and can be derived through the discrete calculation of Eq. (17). The radial power spectrum of the generated phase screen is compared with the theoretical value of Eq. (4), as shown in Fig. 5. The associated parameters are $M = 3$, $N_x' = N_y' = 3$, and $\Delta f_1 = 2\ \mathrm{m}^{-1}$. From Fig. 5, the power spectrum matches the theoretical turbulence very well, which represents a very accurate phase screen.

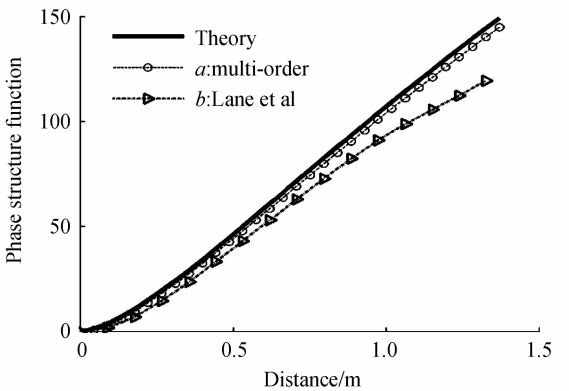

Fig. 4 Phase structure functions of multi-order frequency grid method and method presented by Lane et al. in Ref. 10

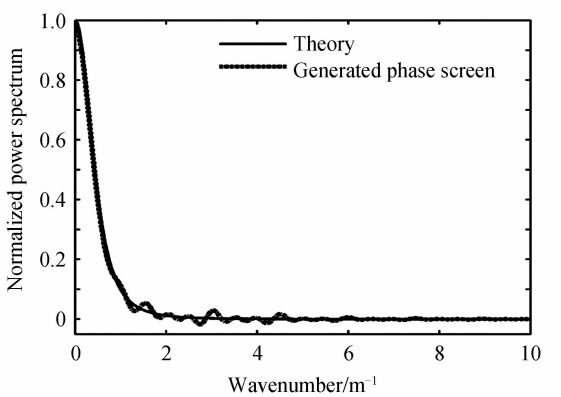

Fig. 5 Power spectrum of generated phase screen compared with theory

Two sample realizations of random phase screen are demonstrated in Fig. 6(a) and (b). The turbulence parameters are $r_0 = 0.1$ m and $L_0 = 10$ m. The parameters of the frequency grids of two random phase screens are selected as $M = 1$, $N_x' = N_y' = 1$, and $\Delta f_1 = 2\ \mathrm{m}^{-1}$ in Fig. 6(a), and $M = 3$, $N_x' = N_y' = 3$, and $\Delta f_1 = 2\ \mathrm{m}^{-1}$ in Fig. 6(b), respectively. The overall slopes in the random screens reflect the low frequency components, which induce the tilt effect of turbulence on the wavefront. In Fig. 6(a), the frequency grids are not subdivided and the slope in the phase screen is not evident, which means the low frequency components are not sampled adequately. In Fig. 6(b), the frequency grids are subdivided and the slope in the phase screen is so significant, which reflects that the low frequency components of turbulence are well

sampled.

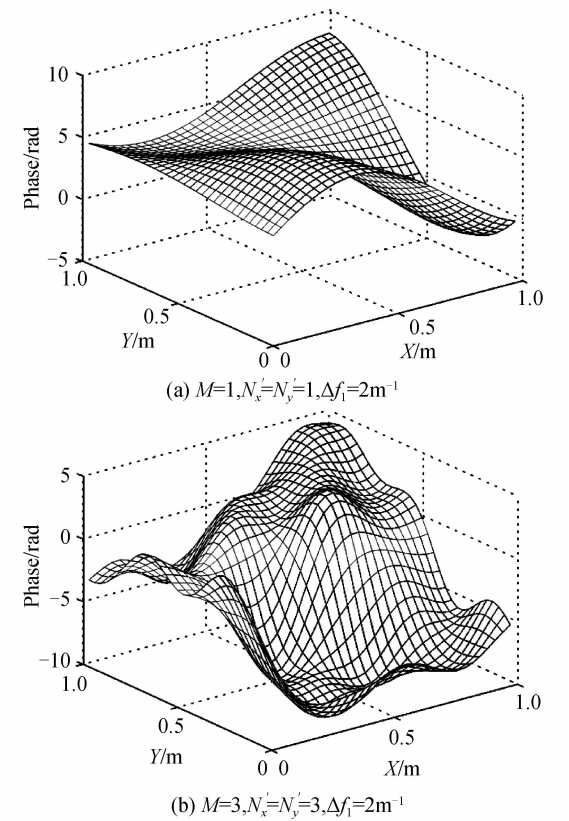

Fig. 6 Two generating random phase screens

The results show that the phase structure function and the power spectrum of phase screen can approach to respective theoretical values with suitable grid dividing and suitable combined parameters, and generated random phases can contain sufficient low frequency components by adopting proper parameters. These prove that low frequency components can be sampled appropriately in our multi-order frequency grid dividing method, which is based on subharmonic principle.

For a conventional method of inversely power spectrum, a FFT-based operation requires generating a quite large phase screen to contain effective low frequency components (the screen size should be at least five times of outer scale L_0), hence the computing amount could be so large. Relatively, our method of multi-order frequency grids (as a kind of subharmonic approach) can generate an accurate phase screen (which is not required to be very large) fast and efficiently. Although the method based on Zernike polynomials can produce Kolmogorov turbulence accurately, it is restricted to a circular screen. For simulating the effect of turbulence moving across the wavefront, it is more convenient to generate a phase screen defined on rectangular Cartesian coordinates.

In our method of multi-order frequency grid subdiving based on the subharmonic principle, since the frequency spaces for multiple orders are different and irregular, the particularly low frequency space cannot be satisfied simultaneously in the frequency range which contributes most to turbulent spectrum. In general, a phase screen within the size of 10m×10m can be generated accurately. If a large amount of frequency grids is adopted in one certain order, a large phase screen may be produced. However, the computing amount will increase in this case and the advantage of this subharmonic method as a low frequency compensation to the traditional FFT-based phase screen is degraded. Our method is suitable to generate a relative small phase screen for simulating the effect of turbulence on the wavefront of a beam. The above mentioned examples show the case of generating a square screen using our method. Note that a rectangular phase screen can also be generated by adopting different parameters along two different directions. It is not efficient to generate a very long phase screen because of the restriction of the screen size.

The simulations for our method are based on the modified Von Kármán spectrum of Eq. (1), which is a modified spectrum of Kolmogorov turbulence. In our method, the phase screen can also be generated by use of other modified spectrums of Kolmogorov turbulence, like Hill spectrum, and the modified spectrum by Andrews and Philips[19]. Moreover, our method can be used to generate non-Kolmogorov spectrum, which is statistically differently from Kolmogorov turbulence. Some statistical terms of the phase screen such as phase structure function and power spectrum may not be directly obtained from 2D autocorrelation function. However, these statistical characteristics can be obtained through evaluating the ensemble average of random phases, by Monte Carlo simulation.

4 Conclusion

A subharmonic method based on the multi-order frequency grid dividing was proposed for generating turbulent phase screen, which can sufficiently compensate the low frequency components lost in the FFT-based screen. Frequency grids for phase screen are firstly divided into multiple orders, and then the frequency grids for every order are further subdivided. In this method, since frequency grids are divided more finely according to the power spectrum of atmospheric turbulence in frequency domain, the generated phase screen can be accurate. The phase structure function and the power spectrum are selected as two references to study the accuracy of the generated phase screen. The modified Von Kármán spectrum of atmospheric turbulence which includes the outer scale L_0 is

employed. For numerical simulation, the outer scale of $L_0 = 10$ m and atmospheric coherence length of $r_0 = 0.1$ m are selected. The accuracy of the simulated phase screen is related to the grid order number M, the frequency space before subdividing Δf_{x1} and Δf_{y1}, and the grid point number of each order $N_x' \times N^{y'}$. The results show that the phase structure function and the power spectrum can be quite close to the theoretical result. The overall slope in the realization of random phase screen reflects that the low frequency components can be well sampled in the screen for proper parameters. In summary, the phase screen generated by the proposed method can be quite accurate while keeping a fast implementation.

References

[1] DIOS F, RECOLONS J, RODRiGUEZ A, *et al*. Temporal analysis of laser beam propagation in the atmosphere using computer-generated long phase screens[J]. *Optics Express*, 2008, **16**(3): 2206-2220.

[2] NISTAZAKIS H E, TSIFTSIS T A, TOMBRAS G S. Performance analysis of free-space optical communication systems over atmospheric turbulence channels [J]. *Iet Communications*, 2009, **3**(8): 1402-1409.

[3] ZHAI Chao, WU Feng, YANG Qing-bo, *et al*. Simulation research of laser beam atmospheric propagation in free-space optical communication[J]. *Chinese Journal of Lasers*, 2013, **40**(5): 0505004 - 1-6.

[4] PARAMONOV P V, VORONTSOV A M, KUNITSYN V E. A three-dimensional refractive index model for simulation of optical wave propagation in atmospheric turbulence[J]. *Waves in Random and Complex Media*, 2015, **25**(4): 556-575.

[5] WU H, SHENG S, HUANG Z, *et al*. Study on beam propagation through a double-adaptive-optics optical system in turbulent atmosphere[J]. *Optical and Quantum Electronics*, 2013, **45**(5): 411-421.

[6] ZOCCHI F E. A simple analytical model of adaptive optics for direct detection free-space optical communication[J]. *Optics Communications*, 2005, **248**: 359-374.

[7] YAN H X, LI S S, ZHANG D L, *et al*. Numerical simulation of an adaptive optics system with laser propagation in the atmosphere[J]. *Applied Optics*, 2000, **39**(18): 3023-3031.

[8] FLECK J A, MORRIS J R, FEIT M D. Time-dependent propagation of high energy Laser beams through the atmosphere[J]. *Applied Physics*, 1976, **10**(2): 129-160.

[9] HERMAN B J, STRUGALA L A. Method for inclusion of low-frequency contributions in numerical representation of atmospheric turbulence[C]. SPIE, 1990, **1221**: 183-192.

[10] LANE R G, GLINDEMANN A, DAINTY J C. Simulation of a Kolmogorov phase screen[J]. *Waves Random Media*, 1992, **2**(3): 209-224.

[11] JOHANSSON E M, GAVEL D T. Simulation of stellar speckle imaging[C]. SPIE, 1994, 2200: 372-383.

[12] ZHANG Bao-dong, QIN Shi-qiao, WANG Xing-shu. Accurate and fast simulation of Kolmogorov phase screen by combining spectral method with Zernike polynomials method [J]. *Chinese Optics Letters*, 2010, **8**(10): 969-971.

[13] CARBILLET M, RICCARDI A. Numerical modeling of atmospherically perturbed phase screens: new solutions for classical fast Fourier transform and Zernike methods[J]. *Applied Optics*, 2010, **49**(31): G47-G52.

[14] XIANG J. Accurate compensation of the low-frequency components for the FFT-based turbulent phase screen[J]. *Optics Express*, 2012, **20**(1): 681-687.

[15] XIANG J. Fast and accurate simulation of the turbulent phase screen using fast Fourier transform [J]. *Optical Engineering*, 2014, **53**(1): 016110.

[16] SEDMAK G. Implementation of fast-Fourier-transform-based simulations of extra-large atmospheric phase and scintillation screens[J]. *Applied Optics*, 2004, **43**(23): 4527-4538.

[17] WANG Jian-ye, RAO Rui-zhong, LIU Xiao-chun. Comparison of experimental study of atmospheric coherence length[J]. *Chinese Journal of Lasers*, 2005, **32**(1): 64-66.

[18] ASSEMAT F, WILSON R W, GENDRON E. Method for simulating infinitely long and non stationary phase screens with optimized memory storage[J]. *Optics Express*, 2006, **14**(3):988-999.

[19] ANDREWS L C, PHILLIPS R L. Laser beam propagation through random media[M]. 2nd ed. Washington USA: SPIE Press, 2005: 67-72.